Title: Proteome analysis of vitreous humor in retinal detachment using two different flow-charts for protein fractionation

Authors: Leonor M. Gaspar, Fátima M. Santos, Tânia Albuquerque, João P. Castro-de-Sousa, Luís A. Passarinha, Cândida T. Tomaz

PII: S1570-0232(17)31064-4
DOI: http://dx.doi.org/doi:10.1016/j.jchromb.2017.07.049
Reference: CHROMB 20726

To appear in: *Journal of Chromatography B*

Received date: 14-6-2017
Revised date: 24-7-2017
Accepted date: 27-7-2017

Please cite this article as: Leonor M.Gaspar, Fátima M.Santos, Tânia Albuquerque, João P.Castro-de-Sousa, Luís A.Passarinha, Cândida T.Tomaz, Proteome analysis of vitreous humor in retinal detachment using two different flow-charts for protein fractionation, Journal of Chromatography Bhttp://dx.doi.org/10.1016/j.jchromb.2017.07.049

Proteome analysis of vitreous humor in Retinal Detachment using two different flow-charts for protein fractionation

Leonor M. Gaspar[1,2], Fátima M. Santos[1,2,3*], Tânia Albuquerque[1], João P. Castro-de-Sousa[4], Luís A. Passarinha[1,3], Cândida T. Tomaz[1,2#]*

[1] CICS-UBI - Health Sciences Research Centre, University of Beira Interior, 6201-506 Covilhã, Portugal

[2] Chemistry Department, Faculty of Sciences, University of Beira Interior, 6201-001 Covilhã, Portugal

[3] Laboratory of Pharmacology and Toxicology - UBIMedical, University of Beira Interior, 6200-284, Covilhã, Portugal

[4] Ophthalmology Service, Leiria Hospital Center, 2410 Leiria, Portugal

*The authors contributed equally to this work

Corresponding author:

Cândida Tomaz, Ph.D.

CICS-UBI – Health Sciences Research Centre, University of Beira Interior

6201-001 Covilhã, Portugal

E-mail: ctomaz@ubi.pt

Fax: +351 275 329 099

Telephone: +351 275 242 021

Highlights

- Two fractionation strategies were proposed for the vitreous proteome analysis in retinal detachment.
- A total of 127 proteins were identified in vitreous of patients with retinal detachment.
- From the proteins identified in vitreous, 68 had not yet been found in previous studies.
- Bidimensional fractionation is more suitable to increase the coverage of vitreous proteome.

ABSTRACT

The deeper understanding of retinal detachment (RD) pathogenesis may improve the visual outcome after surgery. Given the main role of the vitreous in retinal eye diseases, two strategies were explored to identify its proteome in RD. Fractionation techniques such as anion exchange chromatography (IEX) and SDS-PAGE combined with MALDI-TOF/TOF analysis allowed to identify 127 proteins in vitreous of RD patients. From these proteins, 19 were identified using only the IEX fractionation strategy, and 117 using a bidimensional (IEX and SDS-PAGE) fractionation. Of these proteins, 68 had not yet been found in other vitreous proteomic studies. The fractionation with IEX and SDS-PAGE largely improved the number of identified proteins proving that it is crucial to combine several methodologies to cover vitreous proteome.

ABBREVIATIONS

AB, Ammonium Bicarbonate; ACN, Acetonitrile; GO, Gene Ontology; IEX, Ion-exchange Chromatography; pI, Isoelectric Point; LC-ESI-MS/MS, Nano-liquid Chromatography-electrospray Ionization Mass Spectrometry; MALDI-TOF-MS, Matrix-Assisted Laser Desorption Ionization/Time-of-Flight Mass Spectrometry; RD, Retinal Detachment; RRD, Rhegmatogenous Retinal Detachment, SDS-PAGE, Sodium Dodecyl Sulphate Polyacrylamide Gel Electrophoresis; STRAP 1.5, Software Tool for Rapid Annotation of Proteins; STRING 10, Search Tool for the Retrieval of Interacting Genes/Proteins.

Keywords: Electrophoresis; Liquid chromatography; Mass Spectrometry; Proteomic analysis; Retinal Detachment; Vitreous Humor.

1.1. INTRODUCTION

The human eye is a highly organized and complex organ, responsible for visual perception [1]. It is composed by different fluids and structures that may be subjected to biochemical changes during pathological states of the eye [2]. Vitreous humor is a gel-like fluid that fills the cavity behind the lens and the retinal pigment epithelium (RPE) and helps to stabilize the eye structure. Although vitreous is remarkably stable, it may suffer biochemical, proteomic and structural changes overtime according to the physiological and pathological state of the retina. This occurrence can lead to severe ocular pathologies, such as retinal detachment (RD) [1,3].

RD is an ocular disease characterized by a retinal accumulation of fluid between the neurosensory retina and the underlying RPE [4]. It may result of liquefaction of vitreous due to the weakening of vitreoretinal adhesion, and to alterations of the structure of collagen fibers. When this occurs, vitreous falls upon itself causing the physical separation between the photoreceptor layer and the RPE of the retina, leading to severe and permanent loss of vision [4,5]. Currently, the treatment for RD is exclusively surgical but its combination with new therapeutic may improve the visual outcome after surgery [4]. The suitable management of RD is critical to allow the retinal reattachment after surgery and avoid its evolution for more severe diseases such as proliferative vitreoretinopathy (PVR), characterized by enhanced photoreceptor degeneration [4,6]. Vitreous is a suitable matrix for study RD pathogenesis because, due to its location, its proteome and biochemical properties are directly affected by physiological and pathological conditions of the retina [7]. Therefore, it is extremely crucial to explore the vitreous proteome in the rhegmatogenous RD (RRD), the less severe form of RD, in order to make advances in the earlier diagnosis, prognosis, and improvement of visual outcome of the patients after surgery [4,6].

Although the application of proteomics technology in ophthalmic research is much more frequent nowadays [8], there are only a limited number of publications about RD [6,9,10]. In 2008, Shitama and colleagues observed substantially higher expression levels of proteins, such as pigment epithelium derived factor and proapolipoprotein A1 in RD, when compared to other ocular diseases [9]. Yu and colleagues found 516 proteins in vitreous of RRD patients with PVR using SDS-PAGE and reversed-phase liquid chromatography tandem mass spectrometry [10]. More recently, Wu and co-workers

identified 750 proteins by iTRAQ-mass spectrometry, from which 103 were found differentially expressed in RD with choroidal detachment when compared with RD [6].

Many researchers [11–18] have contributed to the enrichment of our knowledge about human vitreous proteome in several ocular pathologies, using different techniques, as displayed in Table 1. The overview of proteomic strategies applied in the last years emphasize that no individual technology can cover completely the vitreous proteome. So, as the diversity and complexity of the human vitreous proteome is overwhelming, it is important to take into consideration all reported studies to know the entire proteome and understand its change in several pathologic environment [19].

The present study aims to characterize the vitreous proteome of patients with RRD, which is the most common type of RD and is characterized by a full thickness retinal break [4]. For this purpose, vitreous samples from RRD patients, with ages comprised between 26 and 82 years old, were pooled together and analyzed using two different approaches, with and without SDS-PAGE, according to the experimental workflow represented in Figure 1. The first approach included protein fractionation through ion-exchange chromatography (IEX) and identification of the target fractions by MALDI-TOF/TOF. Alternatively, in the second approach, a SDS-PAGE step was introduced after the IEX to improve the fractionation level of vitreous proteins before its identification by MALDI-TOF/TOF.

1.2. MATERIALS AND METHODS

1.2.1. Vitreous sample collection

All vitreous samples were obtained via pars plana vitrectomy at Ophthalmology service of Leiria Hospital Center (Portugal). This study was conducted according to the principles of the Declaration of Helsinki. The sample collection protocol was approved by the hospital ethics committee and an informed consent was obtained from all patients. Characteristics of patients, including age at presentation, sex and disease classification are summarized in Table 2. Vitreous samples contaminated with plasma and associated with other diseases were excluded. Samples from patients subjected to previous intraocular surgeries (including vitrectomy, glaucoma surgery and laser coagulation), intravitreal drug treatments or with other vitreoretinal diseases were also excluded. Vitreous samples from 25 patients with RRD were selected, with ages ranging between 26 and 82. Undiluted samples (500-1000 μL) were collected in sterilized tubes during

surgical procedure, placed on ice immediately and stored at -80ºC until further processing.

1.2.2. Sample preparation

Vitreous samples were centrifuged at 18 620 x g for approximately 10 min at 4ºC, to separate the structural component from the soluble phase. Total protein concentration was measured by Pierce™ BCA Protein Assay Kit (Thermo Scientifics, USA) according to the kit manufacturer's protocol, using BSA as standard and calibration control samples (125-8000 µg/mL). In order to exclude samples with plasma contamination, hemoglobin levels were measured using Hemoglobin Colorimetric Assay Kit (Cayman Chemical, Michigan, USA), following the kit manufacturer's protocol. Then highly abundant proteins, such as human serum albumin and IgG were depleted from vitreous using a HiTrap™ Albumin & IgG Depletion 1 mL column (GE Healthcare, Uppsala, Sweden). Briefly, the depletion was performed at room temperature in an ÄKTA Pure system with UNICORN 6 software (GE Healthcare, Uppsala, Sweden) equipped with a 2 mL injection loop. All buffers pumped in the system were prepared with Mili-Q system water, filtered through a 0.20 µm pore size membrane (Schleicher Schuell, Dassel, Germany) and degassed ultrasonically. Vitreous samples (0.5 to 4 mg) were loaded in column, previously equilibrated with 20 mM sodium phosphate, 0.15 M NaCl at pH 7.4, at a flow rate of 1 mL/min. After the elution of low abundant proteins, the mobile phase conditions were changed to 0.1 M glycine buffer at pH 2.7 to allow the elution of highly abundant proteins. In all chromatographic runs, conductivity, pH, and absorbance, at 280 and 214 nm, were continuously monitored. The collected samples were concentrated and desalted using Vivapsin 6 with a 3.000 MW cut-off, and stored at -20ºC. Depleted samples were pooled together and concentrated to a volume of 2 mL before fractionation by IEX.

1.2.3. Protein fractionation by Ion-exchange chromatography

Ion-exchange chromatography was performed at room temperature in an ÄKTA Pure, equipped with a 500 µL injection loop. Proteins were fractionated according to their isoelectric point (pI) using a HiScreen™ Capto™ Q 4.7 mL column (GE Healthcare, Uppsala, Sweden), containing a strong anion exchanger quaternary ammonium coupled to Sepharose (Q-Sepharose®). Buffer A was prepared by combining 20 mM L-histidine, 20 mM ethanolamine, 20 mM di-ethanolamine, 20 mM tri-ethanolamine, and 20 mM Tris and adjusting the pH to 10 using sodium hydroxide. Buffer B was prepared likewise but by adding 5 mM sodium chloride and adjusting the pH to 5 using chloridric acid. Detailed

description of buffers is presented in supplementary Table S1. Buffers were prepared with Mili-Q system water, filtered through a 0.20 μm pore size membrane (Schleicher Schuell, Dassel, Germany) and degassed ultrasonically. Samples (2-4 mg) were injected onto the column, previously equilibrated with buffer A, at a flow rate of 1.5 mL/min. In order to promote a gradual elution of adsorbed proteins, a linear pH gradient until 100% of buffer B was applied during 15-20 CV, at the same flow rate. The absorbance was continuously monitored at 280 nm, as well as conductivity and pH. Fractions of 1.8 mL were collected and evaporated to a volume near 200 μL, at room temperature, using a UNIVAPO Rotational Vacuum Concentrator 100ECH, and stored at 4ºC until further analysis.

1.2.4. Protein separation by SDS-PAGE

The fractions obtained from IEX were pooled according to their pI and extracted using methanol/chloroform (4:1, v/v) in 3 volumes of water. Each resulting mixture was centrifuged for 5 min at 15 000 x g. The hydrophilic phase was removed and 3 volumes of water were added and the mixture was centrifuged for 10 min at 18 620 x g. The supernatant was removed and the pellet was dried. After the precipitation, the pellet was solubilized with a suitable buffer (150 mM NaCl, 50 mM tris, 1 mM $MgCl_2$, 2% CHAPS, pH 8.0) and each 10 μL of solubilized sample was supplemented by adding 3.5 μL of loading buffer (100 mM tris-HCl (pH 6.8), 4% (w/v) SDS, 0.01% bromophenol blue (w/v), 0.2% glycerol (v/v), 0.02% β-mercaptoethanol (v/v)). Afterwards, proteins were denatured by boiling samples for 5 min at 100ºC, and samples were loaded and run on 12.5% resolving acrylamide gel at 150 V using Amersham SE260 Mighty Small II Deluxe Mini Vertical Electrophoresis Unit system, with a running buffer containing 25 mM tris, 192 mM glycine, 0.1% (w/v) SDS. After electrophoresis, gels were stained using "Blue Silver", a modified colloidal Coomassie Brilliant Blue solution, according to the experimental protocol of Candiano and co-workers [20]. The Coomassie-stained gels were also subjected to a densitometric scan on ImageScanner III obtained from GE Healthcare Life Sciences (Uppsala, Sweden).

1.2.5. In-Gel Tryptic Digestion

Each lane on acrylamide gels was cut into slices of 1-1.5 mm, which were destained with 50% acetonitrile (ACN) and 50 mM ammonium bicarbonate (AB) and dehydrated with ACN. Afterwards, proteins were reduced and alkylated with 10 mM dithiothreitol at 56ºC for an hour and 55 mM iodoacetamide at room temperature for 30 min, respectively. Gel slices were rehydrated in ice, for an hour, with 30 μL of 10 ng/μL trypsin prepared in

digestion solution (25% AB, 9% ACN). After the absorption of trypsin solution, gel slices were covered with digestion solution and proteins were digested overnight at 37ºC. Lastly, the tryptic peptides were firstly extracted with 0.1% TFA in water (37ºC/15min) and then with 0.1% TFA in 50% ACN (37ºC/15min). The extracted tryptic peptides were dried by vaccum centrifugation at room temperature.

1.2.6. In-solution Tryptic Digestion

Each protein fraction obtained by IEX was pooled together according to pH range. Proteins were reduced and denatured with 50 mM Tris-HCl (pH 8), 5 mM dithiothreitol and 8 M urea at final protein concentration of 1 mg/mL. The solubilized samples were incubated at 37ºC for 60 min and, then, 50 mM NH_4HCO_3 (pH 7.8) was added to decrease the urea concentration to less than 1 M. For in-solution digestion, MS grade trypsin (1ug/µL stock) was added in a trypsin:protein ratio of 1:30. The digestion reaction was incubated at 37ºC for at least an hour and stopped with 5% formic acid.

1.2.7. MALDI-TOF/TOF analysis

Before spotting the tryptic peptides into MALDI plate, peptide samples were clean-up with Millipore® Zip-tip C18 0.1-10 µL pipette tips (Molsheim, France). For sample cleaning, dried samples were acidified by solubilizing peptides with 1% TFA, at pH lower than 3. Zip-tip pipette tips were regenerated 5 times using ACN and equilibrated 10 times with 0.1% TFA in LC-MS grade water. After equilibration, tryptic peptides were loaded by careful aspiration and disposal of samples. Using 0.1% TFA in LC-MS grade water, tryptic peptides adsorbed in tips were washed 3 times and eluted in 5 µL of 80% ACN with 0.1% TFA solution. Then, desalted and concentrated tryptic peptides were analyzed by MALDI-TOF/TOF. The standards were a mixture of CalMix 1 and CalMix 2, from AB SCIEX Peptide Mass Standard Kit (Massachusetts, USA). Samples were prepared by combining 5 µL of clean-up peptide samples with 5 µL of CHCA matrix solution (5 mg/mL), and were analyzed on 4800 plus MALDI-TOF/TOF analyzer (Applied Biosystems), equipped with a 355 nm laser. All spots were initially analyzed in a positive MS mode in the range 800 to 4000 m/z by averaging 1500 laser spots. The eight more intense MS ions per spot that meet the precursor criteria (200 ppm fraction-to-fraction precursor exclusion, S/N ratio >25) were selected for subsequent MS/MS analysis. All MS/MS data were acquired using 1 keV collision energy with a total of 1500 laser shots per spectrum. Peak lists were export to a MGF file using the function Peaks to Mascot 4000 Series Explorer™ Software (Applied Biosystems).

1.2.8. Data analysis

Mass spectrometry data was processed using both MASCOT and Paragon search engines incorporated in ProteinPilot™ Software 4.5 (AB SCIEX, Massachusetts, USA), under a 95% confidence. Each peak list was searched against the *Homo sapiens* UniprotKB canonical & isoform reviewed database (48,355 entries) downloaded from Swiss-Prot *Homo sapiens* in FASTA format. In Paragon, the search parameters were cysteine modification by methyl-methanethiosulfonate, digestion of peptides with trypsin and default biological modification settings [21]. In MASCOT, search parameters were set as follows: enzyme – trypsin, variable modifications - carboxymethyl (C), oxidation (M), and peptide mass tolerance – 0.1 Da. In this study, protein scores of 1.3/1.3 and 56 were used as a cutoff for protein identification in Paragon and MASCOT. After protein identification, online tool STRING 10 (Search Tool for the Retrieval of Interacting Genes/Proteins) (http: //string-db.org) was used to find protein clusters with shared protein-protein associations and to get an overall overview of the proteins found in RRD vitreous. Identified proteins were analyzed according to Gene Ontology (GO) terms for biological process, cellular component and molecular function using STRAP 1.5 (Software Tool for Rapid Annotation of Proteins).

1.3. RESULTS

1.3.1. Patient characterization and sample pooling

Vitreous from 25 individuals (n=18 males; n=7 females) with ages between 26 and 82 years old were collected. As previously referred, characteristics of all patients, including age at presentation and gender, are summarized in Table 2. For fractionation by IEX, depleted samples were pooled instead of performing individual assays. The main advantage of pooling is promote an overall decrease of the sample variability, due to differences between individual samples, making the global sample more representative for the study of the target ocular pathology [22]. Also, due to the restrict number of samples, pooling is considered a suitable strategy to increase the available protein quantity.

1.3.2. Experimental set-ups for vitreous proteome analysis

In this work, two experimental set-ups based on techniques, such as IEX and SDS-PAGE, were explored to analyze the proteome of vitreous from RRD patients (Figure 1). In the first methodology, before the protein identification by MALDI-TOF/TOF, the vitreous samples were fractionated only by IEX, using an anion exchanger column (Q-Sepharose)

and a mobile phase with different pH. The typical chromatogram (Figure 2A) showed that the majority of proteins are eluted at pH ranging between 5.5 and 8, which means they present low pI. Since these samples were still quite complex for the analysis by MALDI-TOF/TOF, in the second approach the IEX methodology was combined with SDS-PAGE (Figure 2B) before its identification by MS, to improve the fractionation of vitreous proteins, especially the ones that have low pI.

1.3.3. Vitreous proteome and gene ontology classification

The MS/MS data was evaluated using the following criteria: the score must be higher than 1.3 and 56, respectively, for Paragon and MASCOT search engines and the proteins should be identified with ≥2 peptides. The number of proteins identified by each experimental strategy is summarized in Table 3. Also, the complete list of all detected proteins in RRD vitreous is provided in supplementary Table S2 together with their accession number, gene, score, sequence coverage, protein mass, and number of identified peptides. Regarding the first methodology, which combined fractionation by IEX and MS analysis, only 19 proteins were identified, under a 95% confidence, with ≥2 peptides and scores above 56 for MASCOT and 2 for Paragon. Nevertheless, a total of 112 proteins with ≥1 peptide were found with a score higher than 1.3 using Paragon algorithm. In the second strategy, with SDS-PAGE as an additional step, the number of detected proteins was increased to 117 using the same search engines, under a 95% confidence. Using MASCOT, 2257 proteins were found but only 45 were identified with scores above 56. With the algorithm PARAGON, 452 proteins were found with ≥1 peptide but, of these, 79 proteins were identified with ≥2 peptides and scores ≥2. So, using both fractionation approaches, a total of 127 proteins were identified with ≥2 peptides and scores above 56 for MASCOT and 2 for Paragon, but only 9 proteins were identified simultaneously in both strategies. As seen in Table 4, the most of the proteins identified in both strategies is abundant in human vitreous, including hemopexin, prostaglandin-H2 D-isomerase, serotransferrin, transthyretin and keratin proteins (KRT1, KRT9). Their high abundance in vitreous is suggested by the fact that these specific proteins have been identified in many of the previous studies [12,14–16] even using different experimental strategies (supplementary Table S3). Also, many proteins were only identified in the second strategy because they don't fulfil the requirements for protein identification in the first one. Proteins, such as alpha-1-antitrypsin, adenylate cyclase type 8, chondroitin sulfate synthase 3, coiled-coil domain-containing protein 141, collagen alpha-5(VI) chain, DENN domain-containing protein 4C, voltage-dependent R-type calcium channel

subunit alpha-1E, among others, were detected using the first strategy but only with 1 peptide. Also, the score, coverage and number of peptides of the identified proteins were enhanced in the second strategy compared to the first one.

In order to know if some new proteins were identified in vitreous, our data were compared to previous vitreous proteomics reports. Since there is still not much information about proteomic analysis in RRD, the comparison were also made with studies concerning other ocular pathologies [12,14–16]. The complete list of proteins can be assessed in supplementary Table S3. The methodology performed in the present work allowed the identification of 68 vitreous proteins that had not yet been found in other studies. For instance, proteins such as adenylate cyclase type 8, BUD13 homolog (BUD13), and Sialoadhesin (SIGLEC1) were identified for the first time with a high score using the methodology that combines IEX with SDS-PAGE. Despite the low number of proteins that were identified using the first methodology, it was also possible to identify new proteins, such as coiled-coil domain-containing protein 13 and 141, protein asteroid homolog 1, rho-associated protein kinase 2, and UDP-glucuronosyltransferase 2B11. On the other hand, ethylmalonyl-CoA decarboxylase and liprin-alpha-2 (table 4) were newly identified in this study using both strategies. Only 59 of the 127 proteins were simultaneously found in this work and in other reports (supplementary Table S3).

For a deeply knowledge about the biological roles and pathways in which proteins are involved, the 127 proteins were analyzed using the bioinformatics tools STRAP and STRING. STRAP allowed to classify the protein data according to their GO terms for biological process, cellular component and molecular function, as can be accessed in supplementary Table S4 or in pie charts from Figure 3. The classification in terms of biological processes (Figure 3A) showed that 81 and 65 proteins are involved, respectively, in cellular processes and regulation, which includes DNA transcription and its regulation. Indeed, many proteins from the zinc finger family, such as the zinc finger proteins 229, 333, 574 and 808, participate in transcriptional regulation. Some of the proteins involved in the interaction with cells and organisms regulate processes, such as cell, cell-matrix, or focal adhesion. Regarding to molecular functions (Figure 3B), 79 proteins have binding functions and interact with molecules, such as DNA, RNA, proteins and metal ions. Also, 47 of the identified proteins have catalytic activity, including hydrolase and transferase activity. Classification based on cellular component (Figure 3C) showed that the large majority of proteins are localized in the cytoplasm or in nucleus.

To perform a straightforward revision of the given information about the identified proteins, STRING10 was used to generate an overall interaction network, where 65 interactions were established between 53 of the 127 proteins identified in vitreous, as can be seen in Figure 4A. Clusters of densely connected proteins can be observed in the interaction network, meaning that they share common functional associations. These clusters were categorized according the common functions, as represented at different colors in the Figure 4B and in supplementary Table S4. Cluster 1 was classified as actin cytoskeleton organization/muscle contraction and, specifically, rho-associated protein kinase 2 (ROCK2) appears to be involved in the regulation of both processes. In this cluster, myosin proteins (MYH1, MYH3) are responsible by muscle contraction, spectrins (SPTBN2, SPTA1) are major constituents of the cytoskeletal network, and titin, plectin and obscurin are muscle structural components. Proteins from cluster 2 activate signaling pathways via G-protein coupled receptor. Guanine nucleotide-binding proteins (G proteins) are modulators or transducers in various transmembrane signaling systems. Neuroendocrine secretory protein 55 is a G protein involved in hormonal regulation of adenylate cyclase (ADCY8). Cluster 3 is composed by plasma proteins that perform numerous functions including platelet degranulation and activation, tissue remodeling and vesicle-mediated transport. Proteins from cluster 4 are epidermis structural molecules and from cluster 5 are microtubule associated molecules, essential for its movement.

1.4. Discussion

Several approaches for sample fractionation could be applied for reducing the complexity of the entire sample before protein identification by MS [8]. In last years, SDS-PAGE has been one of the predominant methods to achieve this goal in vitreous samples (Table 1) [12,14–16]. In this work, two experimental set-ups, based on techniques such as IEX and SDS-PAGE, were explored to analyze the vitreous proteome of RRD patients.

In the first methodology, which combines the fractionation by IEX and MS analysis, only 19 proteins were identified with more than 1 peptide. The application of SDS-PAGE as an additional step increases the number of identified proteins to 117, with high scores. This bidimensional fractionation promotes the separation of vitreous proteins, the reduction of the sample complexity and, consequently, the increase of the number of identified proteins. Indeed, the fact that only 9 proteins were identified simultaneously in both experimental strategies proves the importance of an improved fractionation strategy for increasing the coverage of human vitreous proteome. In general, the score, coverage

and number of peptides were largely increased using the second strategy. So, the second fractionation by molecular weight appears to allow the recovery of a higher number of peptides, thus increasing the number of proteins identified.

It is also interesting to note that the combination of PARAGON and MASCOT, besides of increasing the number of identified proteins, helps to validate protein identifications from each search engine. Since there is still not much information about proteomic analysis in RRD, our data were compared to previous vitreous proteomics reports concerning other ocular pathologies [12,14–16]. Although the number of vitreous proteins discovered in present study was not too high, 68 of them had not yet been found. Indeed, only 59 from the 127 proteins were simultaneously identified in this work and in other studies (supplementary Table S3). Curiously, newly found proteins correspond to the same family of proteins that have been previously identified in the vitreous. Also, the giant protein Titin was identified using the IEX with SDS-PAGE strategy, indicating that this approach is suitable to analyze large proteins. The analysis and identification of high molecular mass proteins (>100 kDa) is challenging, mainly for gel-based methods, such as bidimensional electrophoresis [19]. It was already reported that the sequence coverage of the identified proteins decreases substantially with the increase of its molecular weight [23].

This study showed that minor alterations in the design of a flow chart for protein extraction in vitreous proteomic analysis, can affect the number/recuperation yield and consequently the identification of target proteins. Due to the complexity of vitreous, it is crucial to combine several proteomic methodologies (LC, SDS-PAGE and MALDI) to achieve a deeper analysis of the complete vitreous proteome in RRD.

By using STRING10 an overall interaction network was observed with 65 interactions between 53 of the 127 proteins identified in vitreous (Figure 4A) that were categorized according common functional associations. The STRAP classification showed that identified proteins are involved in different cellular processes and regulation, as well as, in molecular functions, such as binding and interactions with DNA and RNA. Since some of these proteins could be involved in pathological mechanism of RRD, pilot studies are recommended to use this proteomic strategy for the comprehensive analysis of protein alterations in vitreous of RRD patients in order to provide valuable information for future investigations of this eye disease.

1.5. CONCLUSIONS

In the present work, 127 proteins were identified in vitreous of RDD patients, combining two different fractionation methodologies, such as IEX and SDS-PAGE, followed by MALDI-TOF/TOF. It is important to note that 68 of the identified vitreous proteins had not yet been found in other studies. From these two strategies, the one that combines LC and SDS-PAGE for protein fractionation was suitable to improve the number of proteins identified in vitreous from patients with RDD. This approach can also be applied to analyze large proteins. Furthermore, it was demonstrated that minor alterations in the design of a flow chart for protein extraction in vitreous proteomic analysis, can affect the recovery and, consequently, the identification of target proteins. Thus, due to the complexity of vitreous samples, it is crucial to combine several methodologies (LC, SDS-PAGE and MALDI) in order to cover the complete proteome. In conclusion, the developed strategy allowed the detection of proteins which were not identified using other proteomic strategies. This is a very crucial aspect since the proteins identified in this study could be involved in the pathological mechanism of RRD and may lead to the improvement of the understanding of this retinal disease.

CONFLICT OF INTEREST STATEMENT

The authors declare no conflict of interest.

ACKNOWLEDGMENTS

Santos FM acknowledges a fellowship (CENTRO-07-ST24-FEDER-002014) and a doctoral fellowship (SFRH/BD/112526/2015) from FCT. Gaspar LM acknowledges a fellowship from Novartis Farma-Produtos Farmacêuticos, SA. This work was supported by FEDER funds through the POCI - COMPETE 2020 - Operational Programme Competitiveness and Internationalisation in Axis I - Strengthening research, technological development and innovation (Project POCI-01-0145-FEDER-007491) and National Funds by FCT - Foundation for Science and Technology (Project UID/Multi/00709/2013).

REFERENCES

[1] J.M. Petrash, Aging and age-related diseases of the ocular lens and vitreous body., Invest. Ophthalmol. Vis. Sci. 54 (2013) ORSF54-9. doi:10.1167/iovs.13-12940.

[2] J.P. Monteiro, F.M. Santos, A.S. Rocha, J.P. Castro-de-Sousa, J.A. Queiroz, L.A. Passarinha, C.T. Tomaz, Vitreous humor in the pathologic scope: Insights from proteomic approaches, PROTEOMICS - Clin. Appl. 9 (2015) 187–202. doi:10.1002/prca.201400133.

[3] M. Kodama, T. Matsuura, Y. Hara, Structure of vitreous body and its relationship with liquefaction, J. Biomed. Sci. Eng. 6 (2013) 739–745. doi:10.4236/jbise.2013.67091.

[4] M.-N. Delyfer, W. Raffelsberger, D. Mercier, J.-F. Korobelnik, A. Gaudric, D.G. Charteris, R. Tadayoni, F. Metge, G. Caputo, P.-O. Barale, R. Ripp, J.-D. Muller, O. Poch, J.-A. Sahel, T. Léveillard, Transcriptomic Analysis of Human Retinal Detachment Reveals Both Inflammatory Response and Photoreceptor Death, PLoS One. 6 (2011) e28791. doi:10.1371/journal.pone.0028791.

[5] F. Kuhn, B. Aylward, Rhegmatogenous retinal detachment: a reappraisal of its pathophysiology and treatment., Ophthalmic Res. 51 (2014) 15–31. doi:10.1159/000355077.

[6] Z. Wu, N. Ding, M. Yu, K. Wang, S. Luo, W. Zou, Y. Zhou, B. Yan, Q. Jiang, Identification of Potential Biomarkers for Rhegmatogenous Retinal Detachment Associated with Choroidal Detachment by Vitreous iTRAQ-Based Proteomic Profiling, Int. J. Mol. Sci. 17 (2016) 2052. doi:10.3390/ijms17122052.

[7] M. Angi, H. Kalirai, S.E. Coupland, B.E. Damato, F. Semeraro, M.R. Romano, Proteomic Analyses of the Vitreous Humour, Mediators Inflamm. 2012 (2012) 1–7. doi:10.1155/2012/148039.

[8] A.S. Rocha, F.M. Santos, J.P. Monteiro, J.P. Castro-de-Sousa, J.A. Queiroz, C.T. Tomaz, L.A. Passarinha, Trends in proteomic analysis of human vitreous humor samples, Electrophoresis. 35 (2014) 2495–2508. doi:10.1002/elps.201400049.

[9] T. Shitama, H. Hayashi, S. Noge, E. Uchio, K. Oshima, H. Haniu, N. Takemori, N. Komori, H. Matsumoto, Proteome Profiling of Vitreoretinal Diseases by

Cluster Analysis., Proteomics. Clin. Appl. 2 (2008) 1265–1280. doi:10.1002/prca.200800017.

[10] J. Yu, R. Peng, H. Chen, C. Cui, J. Ba, Elucidation of the pathogenic mechanism of rhegmatogenous retinal detachment with proliferative vitreoretinopathy by proteomic analysis., Invest. Ophthalmol. Vis. Sci. 53 (2012) 8146–53. doi:10.1167/iovs.12-10079.

[11] K. Yamane, A. Minamoto, H. Yamashita, H. Takamura, Y. Miyamoto-Myoken, K. Yoshizato, T. Nabetani, A. Tsugita, H.K. Mishima, Proteome analysis of human vitreous proteins., Mol. Cell. Proteomics. 2 (2003) 1177–87. doi:10.1074/mcp.M300038-MCP200.

[12] K.R. Murthy, R. Goel, Y. Subbannayya, H.K. Jacob, P.R. Murthy, S. Manda, A.H. Patil, R. Sharma, N.A. Sahasrabuddhe, A. Parashar, B.G. Nair, V. Krishna, T. Prasad, H. Gowda, A. Pandey, Proteomic analysis of human vitreous humor, Clin. Proteomics. 11 (2014) 29. doi:10.1186/1559-0275-11-29.

[13] T. Nakanishi, R. Koyama, T. Ikeda, A. Shimizu, Catalogue of soluble proteins in the human vitreous humor: comparison between diabetic retinopathy and macular hole., J. Chromatogr. B. Analyt. Technol. Biomed. Life Sci. 776 (2002) 89–100. http://www.ncbi.nlm.nih.gov/pubmed/12127329 (accessed October 31, 2013).

[14] B.-B.B. Gao, X. Chen, N. Timothy, L.P. Aiello, E.P. Feener, Characterization of the vitreous proteome in diabetes without diabetic retinopathy and diabetes with proliferative diabetic retinopathy., J. Proteome Res. 7 (2008) 2516–25. doi:10.1021/pr800112g.

[15] S. Aretz, T.U. Krohne, K. Kammerer, U. Warnken, A. Hotz-Wagenblatt, M. Bergmann, B. V Stanzel, T. Kempf, F.G. Holz, M. Schnölzer, J. Kopitz, In-depth mass spectrometric mapping of the human vitreous proteome., Proteome Sci. 11 (2013) 10. doi:10.1186/1477-5956-11-22.

[16] T. Kim, S.J. Kim, K. Kim, U.-B. Kang, C. Lee, K.S. Park, H.G. Yu, Y. Kim, Profiling of vitreous proteomes from proliferative diabetic retinopathy and nondiabetic patients., Proteomics. 7 (2007) 4203–15. doi:10.1002/pmic.200700745.

[17] S. Loukovaara, H. Nurkkala, F. Tamene, E. Gucciardo, X. Liu, P. Repo, K. Lehti, M. Varjosalo, Quantitative Proteomics Analysis of Vitreous Humor from

Diabetic Retinopathy Patients, J. Proteome Res. 14 (2015) 5131–5143. doi:10.1021/acs.jproteome.5b00900.

[18] J. Naru, R. Aggarwal, U. Singh, A.K. Mohanty, D. Bansal, N. Mangat, N. Kakkar, N. Agnihotri, Proteomic analysis of differentially expressed proteins in vitreous humor of patients with retinoblastoma using iTRAQ-coupled ESI-MS/MS approach, Tumor Biol. (2016) 1–12. doi:10.1007/s13277-016-5162-3.

[19] K. Chandramouli, P.-Y. Qian, Proteomics: challenges, techniques and possibilities to overcome biological sample complexity., Hum. Genomics Proteomics. 2009 (2009) 22. doi:10.4061/2009/239204.

[20] G. Candiano, M. Bruschi, L. Musante, L. Santucci, G.M. Ghiggeri, B. Carnemolla, P. Orecchia, L. Zardi, P.G. Righetti, Blue silver : A very sensitive colloidal Coomassie G-250 staining for proteome analysis, (2004) 1327–1333. doi:10.1002/elps.200305844.

[21] A.C.L. Len, M.B. Powner, L. Zhu, G.S. Hageman, X. Song, M. Fruttiger, M.C. Gillies, Pilot Application of iTRAQ to the Retinal Disease Macular Telangiectasia, J. Proteome Res. 11 (2012) 537–553. doi:10.1021/pr200889t.

[22] P. Escoffier, L. Paris, B. Bodaghi, M. Danis, D. Mazier, C. Marinach-Patrice, Pooling aqueous humor samples: Bias in 2D-LC-MS/MS strategy?, J. Proteome Res. 9 (2010) 789–797. doi:10.1021/pr9006602.

[23] H. Lim, J. Eng, J.R. Yates, S.L. Tollaksen, C.S. Giometti, J.F. Holden, M.W.W. Adams, C.I. Reich, G.J. Olsen, L.G. Hays, Identification of 2D-gel proteins: A comparison of MALDI/TOF peptide mass mapping to ? LC-ESI tandem mass spectrometry, J. Am. Soc. Mass Spectrom. 14 (2003) 957–970. doi:10.1016/S1044-0305(03)00144-2.

FIGURES

Figure 1. Experimental workflow for vitreous humor proteome analysis using two different strategies: (A) Anion-exchange chromatography (IEX) fractionation (B) IEX and SDS-PAGE fractionation

Figure 2. (A) Chromatogram obtained on protein fractionation of pooled depleted vitreous humor by anion-exchange chromatography (IEX). Fractionation was performed with 20 mM L-histidine, 20 mM Tris, 20 mM Ethanolamine, 20 mM Di-ethanolamine and 20 mM Tri-ethanolamine (pH 10) followed by a decreasing pH gradient with 20 mM L-histidine, 20 mM Tris, 20 mM Ethanolamine, 20 mM Di-ethanolamine and 20 mM Tri-ethanolamine and 5 mM NaCl (pH 5). Blue, dashed green, and pink lines represents the absorbance at 280 nm, the percentage of elution buffer, and the pH, respectively. (B) SDS-PAGE of the samples collected from IEX according to their pI.

Figure 3. Pie charts with the classification of the 127 proteins identified in rhegmatogenous retinal detachment (RRD) by gene ontology for (A) Biological Process, (B) Cellular Compartment, and (C) Molecular Function, according to STRAP software.

Figure 4. (A) Protein-protein interaction network of the 127 proteins identified in rhegmatogenous retinal detachment (RRD). Each color of edge represents a type of action established between proteins in the network, according to the image label. (B) Clusters corresponding to densely connected proteins in the interaction network. Clusters 1 and 2 are significantly related to actin cytoskeleton organization/muscle contraction and to G-protein coupled receptor signaling pathways, respectively. The components of clusters 3, 4 and 5 are associated to plasma, epidermis and microtubules, respectively.

TABLES

Table 1. Proteomic studies developed with vitreous humor matrices in several eye diseases.

Techniques	Identified proteins	Ocular pathology	Report
- Immunoaffinity depletion - SDS-PAGE - LC-MALDI-MS/MS	54 proteins	Proliferative diabetic retinopathy (PDR)	[16]
- 2D-PAGE - MALDI-TOF-MS	56 proteins	Diabetic retinopathy	[13]
- SDS-PAGE - LC-ESI-MS/MS	252 proteins	Proliferative diabetic retinopathy (PDR)	[14]
- IEF - SDS-PAGE - LC-ESI-MS/MS	1111 proteins	Epiretinal gliosis	[15]
- Affinity depletion - SDS-PAGE - LC-MS/MS	1205 proteins	Vitreoretinopathy	[12]
- 2D-PAGE - MALDI-TOF-MS/MS	38 proteins	Proliferative diabetic retinopathy (PDR)	[11]
- LC-MS/MS	2482 proteins	Proliferative diabetic retinopathy (PDR)	[17]
- iTRAQ - ESI-MS/MS	431 proteins	Retinoblastoma	[18]

Electrospray Ionization with tandem Mass Spectrometry (ESI-MS/MS); Isobaric Tag For Relative And Absolute Quantitation (iTRAQ); Isoelectric Focusing (IEF); Liquid Chromatography coupled to Electrospray Ionization with tandem Mass Spectrometry (LC-ESI-MS/MS); Liquid Chromatography coupled to Matrix-Assisted Laser Desorption/Ionization with tandem Mass Spectrometry (LC-MALDI-MS/MS); Liquid Chromatography coupled to tandem Mass Spectrometry (LC-MS/MS); Matrix-Assisted Laser Desorption/Ionization Mass Spectrometry (MALDI-TOF-MS) and tandem Mass Spectrometry (MALDI-TOF-MS/MS); Sodium Dodecyl Sulfate–Polyacrylamide Gel Electrophoresis (SDS-PAGE); Two-Dimensional Sodium Dodecyl Sulfate–Polyacrylamide Gel Electrophoresis (2D-PAGE).

Table 2. Characteristics of patients with Rhegmatogenous Retinal Detachment involved in the study, including age at presentation and gender.

Vitreous sample	Gender	Age
1	Male	72
2	Female	61
3	Male	60
4	Male	74
5	Male	52
6	Female	30
7	Male	80
8	Male	75
9	Male	71
10	Male	50
11	Female	82
12	Male	77
13	Male	59
14	Female	72
15	Male	64
16	Male	74
17	Male	62
18	Male	68
19	Female	49
20	Female	62
21	Male	57
22	Male	66
23	Male	26
24	Male	64
25	Female	76

Table 3. Number of proteins identified in vitreous humor of patients with rhegmatogenous retinal detachment using two experimental set-ups, based on protein fractionation by anionic exchange chromatography (IEX) and SDS-PAGE and protein identification combining MALDI-TOF/TOF and MASCOT/Paragon.

Experimental Set-up	Paragon	MASCOT	Number of newly found proteins	Total Number
LC-MALDI-TOF/TOF	12	13	10	19
LC-SDS-PAGE-MALDI-TOF/TOF	78	45	60	117
	83	50	68	127

Table 4. List of the proteins that were identified in both strategies, IEX-MALDI-TOF/TOF and IEX-SDS-PAGE-MALDI-TOF/TOF.

Accession number	Description	Gene Symbol	Biological Process	Protein mass	Paragon / MASCOT Score	Number of peptides (Paragon/MASCOT)	Coverage
Q9NTX5	Ethylmalonyl-CoA decarboxylase	ECHDC1	Lyase involved in decarboxylation of potentially toxic metabolites	31185	———	———	———
					73*	5*	25.0*
P02790	Hemopexin	HPX	Transport Host-virus interaction	52397	10.00**	9**	23.6**
					257**	4**	17.0**
P35527	Keratin, type I cytoskeletal 9	KRT9	structural constituent of cytoskeleton	62259	4.40**	4**	17.2**
					125**	4**	13.0**
P04264	Keratin, type II cytoskeletal 1	KRT1	structural constituent of cytoskeleton	66173	18.01**	28**	40.5**
					542**	4**	15.0**
O75334	Liprin-alpha-2	PPFIA2	cell-matrix adhesion Neurotransmitter secretion	141049	———	———	———
					58*,**	6*,**	8.0*,**
P41222	Prostaglandin-H2 D-isomerase	PTGDS	Isomerase involved in prostaglandins and thromboxanes synthesis	21247	6.00**	8**	51.6**
					235**	1**	8.0**
Q9BQN1	Protein FAM83C	FAM83C	MAPK signaling	81027	4.00**	2**	6.8**
					———	———	———
P02787	Serotransferrin	TF	Iron transport	77000	22.49**	35**	32.1**
					364**	5**	14.0**
P02766	Transthyretin	TTR	Thyroid hormone binding	15993	8**	6**	53.7**
					204**	4**	40.0**

* Higher score corresponding to the identification using the methodology that combines fractionation by IEX and identification by MALDI-TOF/TOF.

** Higher score corresponding to the identification using the methodology that combines fractionation by IEX and SDS-PAGE and identification by MALDI-TOF/TOF.

Figr-1

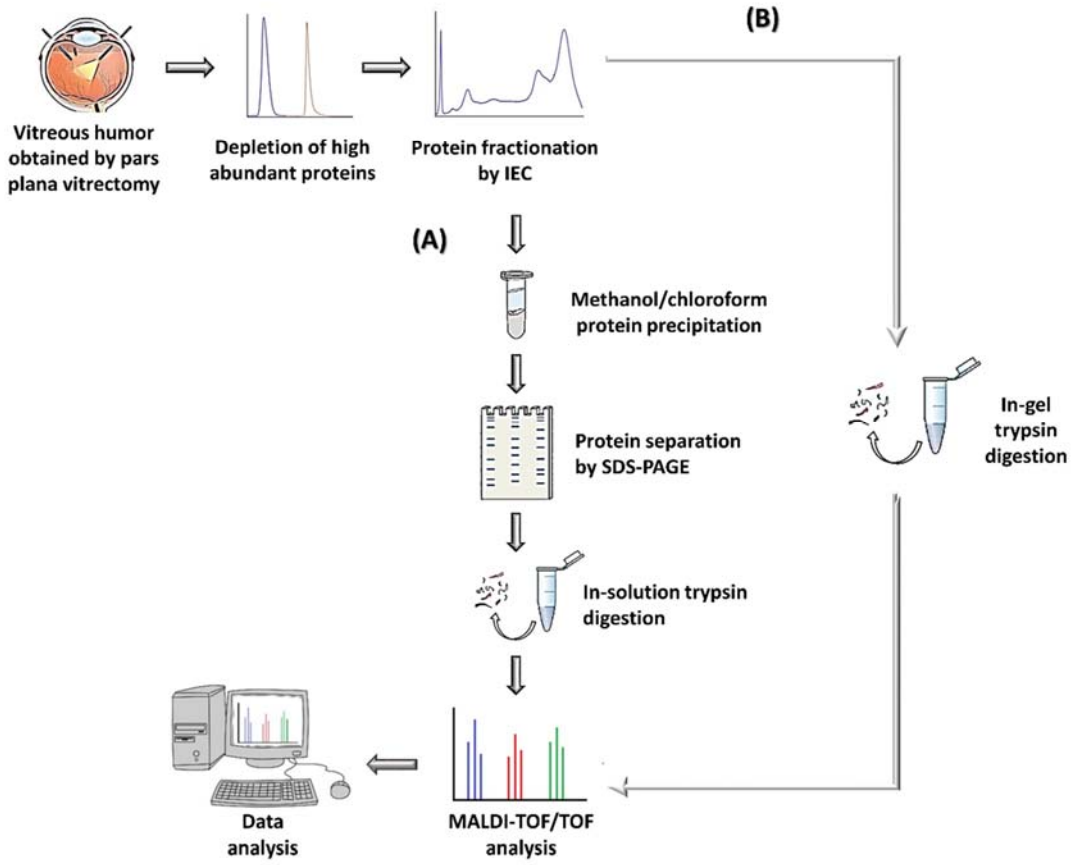

Figr-2

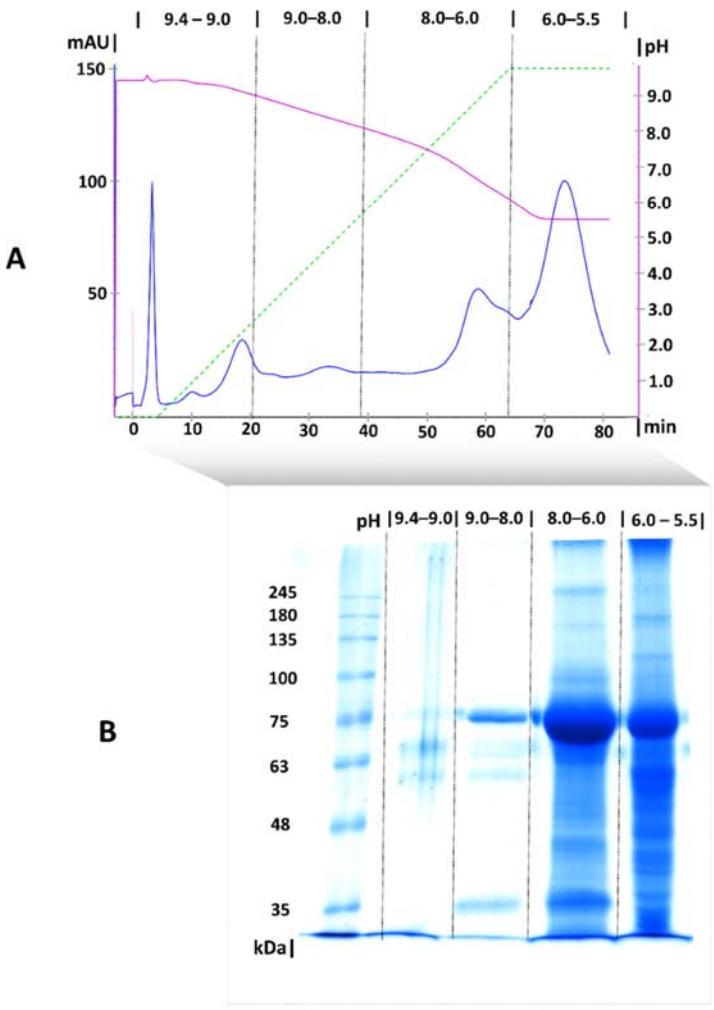

Figr-3

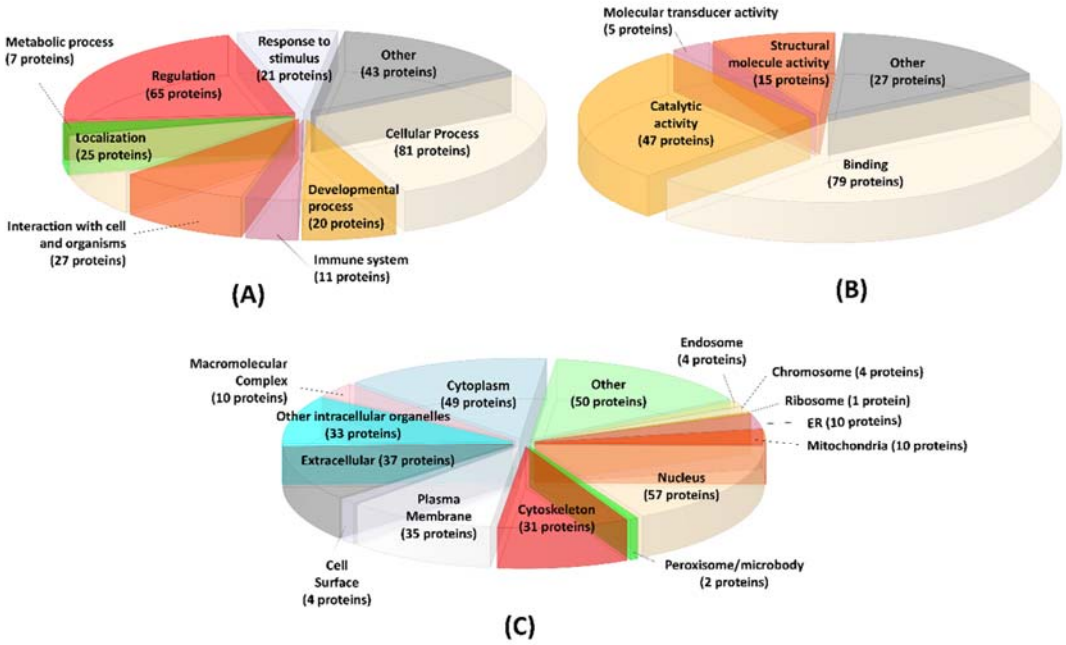

Figr-4